

Analysis and Design of CFRP Steel shear Wall Composites

*Farzad Hatami¹⁾ and Ali Ghamari²⁾

¹⁾ *Institute of Petroleum Industry (R.I.P.I), Tehran, Iran, Hatamif@ripi.ir*

²⁾ *Azad University, Dareshahr branch, Ilam, Iran, ghaytool@yahoo.com*

ABSTRACT

Shear buckling of infill plate of thin Steel Shear Wall (SSW) in few load result pinching in hysteresis loops. Some approaches have been proposed to delay buckling for improving the SSW. These approaches are concrete covering, steel stiffener and use of Load Yield Point (LYP) steel. In the present study, behavior of Composite Steel Shear Wall reinforced (CSSW) with Carbon Fibers Polymer (CFRP) was investigated from both numerical and experimental points. Results indicate that CFRP enhances the structural behavior of steel shear wall. An analytical modeling was carried out to simulate the structural behavior of CSSW. Also several equations were presented in order to draw load-displacement diagrams. This model provides a good understanding of the possible interactions that might take place among different components of the system. It also enables to predict the overall pushover value which is used in nonlinear analysis of CSSW buildings. Finally the results obtained from the proposed model were compared to those of FEM experiments in order to argue the effectiveness and accuracy of the presented method.

Notations	
t_s	Steel plate thickness
G_{12}	CFRP shear module on planes 1-2
F_{ys}	Steel yield strength
G_s	Shear module
E_s	Steel elasticity module
E	Energy absorption
Ω	Over strength

¹⁾ Assistant Professor

²⁾ MS. C., Researcher

1. INTRODUCTION

1.1. Shear buckling of plates

The equation for the elastic buckling load of flat unstiffened panels was first introduced by Bryan (1989). Timoshenko (1961) presented the differential equations for local buckling of rectangular plates. Stein and Neff (1947) carried out some numerical analyses on simply supported plates and produced an accurate diagram for evaluating the shear buckling coefficient of plates. This coefficient, denoted by k_s , is a function of the plate aspect ratio and boundary conditions; see (Bruhn 1973). Budiansky and Connor (1948) produced similar results for clamped plates. Allen and Bulson (1980) published these works and many other studies in a comprehensive review on the background to buckling. The following equations for calculating the critical shear stress of flat rectangular plates are generally accepted and utilized worldwide:

$$\tau_{cr} = \frac{K_s \cdot \pi^2}{12(1-\nu^2)} \left(\frac{t}{b}\right)^2 \quad (1)$$

For plates with all edges simply supported:

$$K_s = 5.34 + \frac{4}{\phi^2} \quad \text{for } \phi > 1 \quad (2)$$

$$K_s = 4 + \frac{5.34}{\phi^2} \quad \text{for } \phi < 1 \quad (3)$$

For plates with all edges clamped:

$$K_s = 8.98 + \frac{5.6}{\phi^2} \quad \text{for } \phi > 1 \quad (4)$$

For values of $\phi < 1$, the same formulae can be applied with the larger side dimension given the designation a , so that $\phi = a/b$ always exceeds unity. For plates with two longitudinal clamped edges and the others simply supported:

$$K_s = -3.44 + 8.39\phi + 2.31/\phi + 5.34/\phi^2 \quad \text{for } \phi < 1 \quad (5)$$

$$K_s = 8.98 + 5.61/\phi^2 - 1.99\phi^{1.99}/\phi^3 \quad \text{for } \phi \geq 1 \quad (6)$$

In recent works, Maquoi and Skaloud (2000) have published a general report on the stability of plated structures such as plate and box girders. They reviewed many issues concerning the simply supported and clamped conditions. Many design specification codes conservatively assume that the juncture is simply supported. Lee et al (1996 and 2002) studied the effects of various boundary conditions. They stated that the real condition is closer to the clamped case in the range of practical design parameters of plate girders, and suggested two relationships.

Bradford (2002) developed a local buckling design chart for the shear buckling coefficient of plate girders that represents the field condition more accurately. Paik and Thayamballi (1996) investigated the normal buckling strength characteristics of elastically restrained steel plates at their edges and developed design formulations for buckling strength as a function of the torsional rigidity of supporting members that provide the rotational restraints along either one set of edges or all four edges.

1.2. Shear Walls

Experimental testing conducted by Lubell (2000), on two single-storey and one four-storey steel shear wall specimens under cyclic quasi-static loading, corroborate these claim. In practice, most designers limit the capacity of a steel plate shear wall to its elastic buckling strength. This practice results not only in a conservative design, but also in an undesirable one, where the columns yield and may buckle before the plate reaches a fraction of its capacity. Plate buckling is not synonymous with failure and, if

the panel is adequately designed, the post-buckling strength can significantly increase the loading capacity. Furthermore, due to the unavoidable out of-plane imperfections, no change in the ultimate load capacity of the panel would be observed (Maquoi and Skaloud 2000).

1.3. Structure of fiber polymers

A composite is defined as a material system consisting of two chemically dissimilar phases that are separated by a distinct interface. In fiber reinforced polymers (FRP), the polymer (or the resin) phase constitutes the binding phase and strong and stiff fibers constitute the fibers phase. Two types of polymers are currently in use: thermosetting polymer and the thermoplastic polymers. The thermosetting polymers are ideally suited for FRP in civil engineering applications. Properties of three commonly used thermosetting polymers (unsaturated polyester, epoxy and vinyl ester) and their typical chemical formulation are given in Table 1. Note that polyester exists both as a thermoplastic polymer as well as a thermosetting polymer, with the latter variety being an unsaturated polymer with at least two double bonds in its monomer [13]. Of the three resins listed in Table 1, polyester is by far the most used. This is due to their low cost and abundant availability. Vinyl ester is, in fact, a type of polyester resin produced by reacting a monofunctional unsaturated acid (methacrylic or acrylic acid) with bisphenol di epoxide. Epoxies are advanced polymeric resins that involve reactions with epichlorohydrin [3], and are more expensive than the polyester or vinyl ester resins. These are used typically in aerospace and defense applications and are characterized

by a highly cross-linked internal structure imparting them a much superior resistance to chemicals and solvents.

High performance carbon Fibers reinforced polymers (CFRP) Because of their unique blend of properties, composites reinforced with high performance carbon fibers find use in many structural applications. However, it is possible to produce carbon fibers with very different properties, depending on the precursor used and processing conditions employed. Commercially, continuous high performance carbon fibers currently are formed from two precursor fibers, poly acrylonitrile (PAN) and mesophase pitch. The PAN-based carbon fiber dominates the ultra-high strength, high temperature fiber market (and represents about 90% of the total carbon fiber production), while the mesophase pitch fibers can achieve stiffness and thermal conductivities unsurpassed by any other continuous fiber.

Table 1. Typical properties of resins used

Resin	Specific gravity	Tensile strength (Mpa)	Tensile modulus (GPa)
Epoxy	1.20 -1.30	55 -130	2.75 - 4.10
Polyester	1.10 -1.40	73 - 81	2.10 - 3.45
Vinyl ester	1.12 -1.32	73 - 81	3.00 - 3.35

These fibers, or their allotropic form graphite, have the most desired properties from civil engineering applications view point. Graphite has a hexagonal structure, a very strong covalent internal bond and very high specific modulus and strength. Unfortunately, graphite has poor properties in the transverse direction and a low shear modulus. The ideal crystal structure of graphite (see Fig. 1) consists of layers in which the carbon atoms are arranged in an open honeycomb network containing two atoms per unit cell

in each layer, labeled A and B. The stacking of the graphene layers is arranged, such that the A and A' atoms on consecutive layers are on top of one another, but the B atoms in one plane are over the unoccupied centers of the adjacent layers, and similarly for the B' atoms on the other plane (Wyckoff 1986). Note that all fibers have a linear elastic response to failure (Sabouri-Ghomi and Ventura 2005).

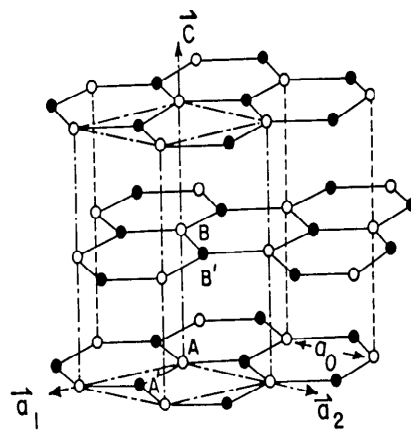


Fig. 1 Crystal Structure of Graphite

1.4. CFRP

Due to unique properties of carbon fibers, composites reinforced with these fibers are used in various structural applications. The properties of carbon fibers greatly differ, depending on processing conditions and the precursor type.

Carbon fibers and their allotropic forms (e.g. graphite) possess the desired properties for civil engineering applications. Graphite has a hexagonal structure and a very strong covalent bond. It also exhibits considerably high specific modulus and strength values. However, graphite possesses a low shear modulus and also poor properties along the transverse direction (winningpen 2001).

2. EXPERIMENTAL STUDY

For this step, 2 experimental specimens were prepared and tested. Both specimens are connected to the rigid frame. The specimens are cyclically loaded as shown in Table 2. These specimens are steel shear wall and steel shear wall composited with CFRP layer. Double I shape steel section that formed box section (2IPE200) strengthened by 12 mm steel plate on both flanges of beams and columns, are used.

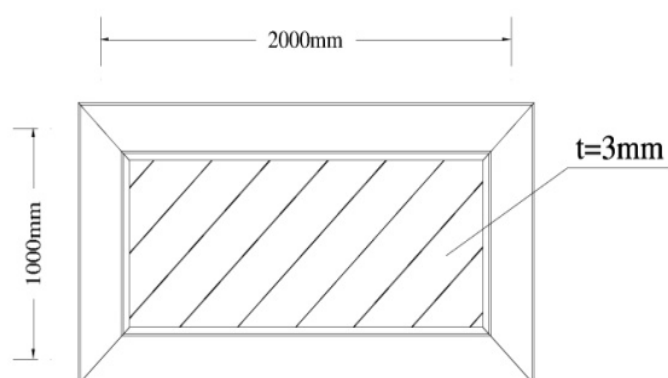


Fig. 2 Dimension of panel

In Composite steel shear wall specimen, there is no connector between the steel plate and the CFRP layer other than epoxy resin. As shown in Fig 2, the specimens dimension are 2 meter width and 1 meter height (Axis to Axis). The test setup is shown in Fig 3. Also yield point and elastic modules of steel material are 235 Mpa and 206 Gpa. And CFRP properties are 240 Gpa elastic modules and 3800 Mpa yield point.

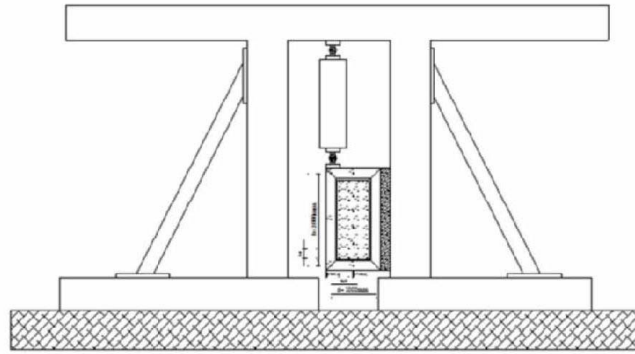


Fig. 3 Test setup

Table 2 Cyclic loading time history

Time(second)		Load (KN)	Shape	Frequencies
Start	End			
0	71	0	Cyclic	0
72	180	300	Cyclic	1/60
181	360	500	Cyclic	1/60
361	540	600	Cyclic	1/60
541	576	600	Cyclic	1
577	720	600	Cyclic	2
721	828	600	Cyclic	3
829	858	600	Rectangular	1
859	878	600	Rectangular	2
879	893	600	Rectangular	3

In steel shear wall specimen, using at least 120 strain gauges and 5 displacement gauges (LVDT) with special cable shield for remittances data of steel frame and plate to data logger and extracted results are used. In sample steel shear wall (SS) the existence of off-plane buckling and post buckling is visible. Maximum value of off-plane displacement is 8mm, which is quite appreciable; considering the thickness of the steel plate (3mm); however in the composite steel shear wall, this value is less than 5mm.

In composite steel shear wall; the steel plate is roughened by sand blasting before being covered with the CFRP layer is then superimposed to both sides of the steel plate laterally and longitudinally. Epoxy resin plus hardener with a certain ratio are used to glue the carbon fiber to the plate and care was taken to eliminate the air bubbles while gluing. Then, the steel plate composited with the CFRP layer is placed inside the steel frame and sandwiched between two layers of pre-prepared L sections flanges, which are fastened together using 6mm bolts with 150mm spacing all around the composite plate.

The existence of the CFRP composite does not get involve in energy transfer of the frame, however it contributes positively in stress distribution over the steel plate. This involvement and distribution will have an increasing effect as the steel plate deformation progresses. All displacement gauges in sample Composite steel shear wall that shows off-plane displacements, indicate that plate behavior is shifting towards post buckling condition, therefore post buckling behavior together with increasing energy absorption and its expansion can be expected to establish as loading increases.

3. NUMERICAL STUDY

The ANSYS Version 11 finite element package is utilized for nonlinear analyses. In reality, the thin infill plates upon mounting are already in a buckled shape due to fabrication process, welding distortion and assemblage. In the incremental nonlinear analysis, initial imperfections proportional to the lowest Eigen-mode shape of elastic buckling is introduced to the plates. Analyses were carried out with the following assumptions:

- The elements are chosen to have elasto-plastic behavior so that off-plane buckling of steel plate could be modeled.

-Convergence criteria for forces and displacements are considered in the models.

- The SOLID element use CFRP layer. It has 6 degrees of freedom having the capability of warping being enforced as the seventh degree of freedom. 3-D SHELL element with four nodes and 6 degrees of freedom per node is chosen for steel materials.

- No gravity loading is done on specimens.

-Von Misses yield theory, which is known to be the most suitable for steel, was used for the material yield criterion.

After several trial and error experiments, the optimum dimensions for the FEM meshes are selected and the shear wall is modeled. Beam and column meshing is designed so that the boundaries of the steel plate meshes coincide with the beam and column mesh to form a common joint. Comparing the results of numerical analyses with the experimental one, numerical models were verified for analysis and modeling of samples with experimented scale. Figs 4&5 compares the load-displacement of the numerical analysis with the experimental specimens in the end of top beam up to 540th second for specimens SS. Note that the jump at the end of the experimental curve is due to entering the loading phase with high frequency. Recording the results similar to other data's because of data logger accuracy was not possible. As shown in Fig 4&5, the load-displacement curves up to 540th second are plotted for comparison the experimental results. Relative area under hysteresis curve of samples CS, S is 0.6206, 0.4177 respectively.

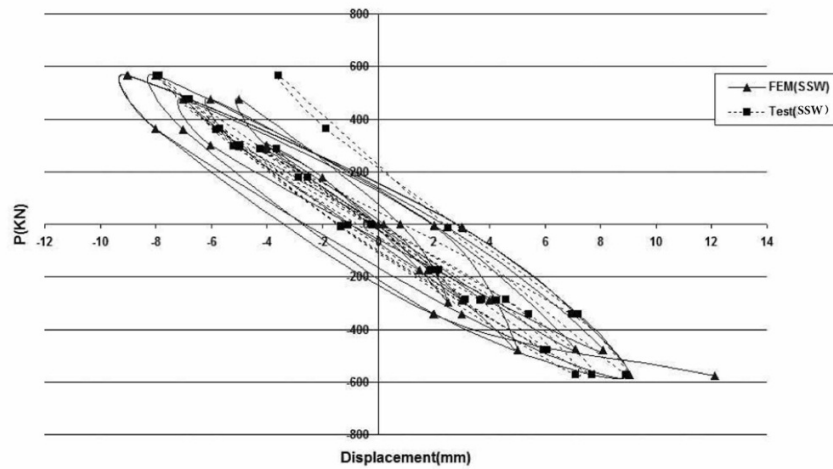


Fig. 4 Comparison of FEM with test (SS model)

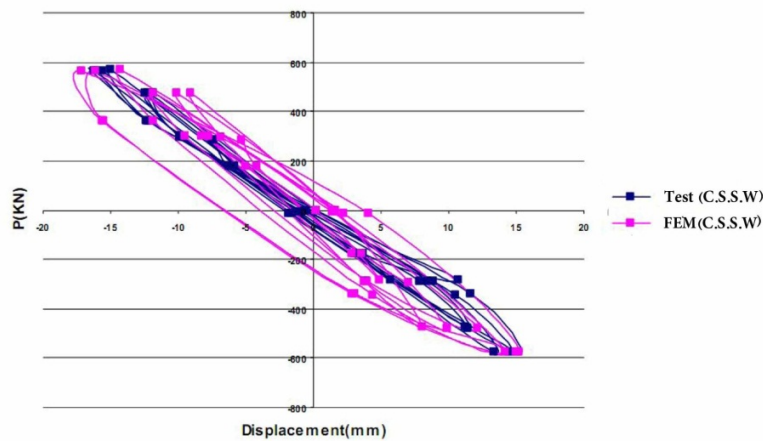


Fig. 5 Comparison of FEM with test (CSS model)

After observing good convergence between the numerical and experimental, many full scale specimens are modeled (see Table 3). In all specimens, 3 m height, 7 mm thickness for steel plate, and 2 mm thickness for fiber polymer were selected.

Also dimension of beam and column were selected as Fig 5. The specimens are named according to the kind of shear wall and dimension and fiber angle. So the first notations refer to the kind of shear wall (SS for steel shear wall and CS for composite shear wall)

and the next two refer to the dimension of panel (bd) and next two refer to angle of fiber polymer.

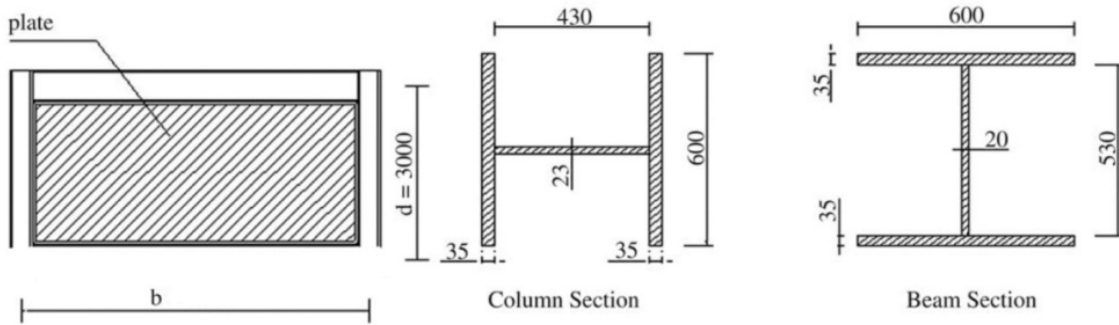


Fig. 5 Specimen geometry

Table 3 Specimens Properties

Specimen	Model	Fiber Angel (Deg)	Panel Width (mm)
SS-33	SSW	---	3000
SS-35	SSW	---	5000
SS-36	SSW	---	6000
CS-33	CSSW	Laterally and longitudinally	3000
CS-35	CSSW	Laterally and longitudinally	5000
CS-36	CSSW	Laterally and longitudinally	6000
CS-33-30	CSSW	30	3000
CS-33-45	CSSW	45	3000
CS-33-60	CSSW	60	3000
CS-33-90	CSSW	90	3000
CS-35-30	CSSW	30	5000
CS-35-45	CSSW	45	5000
CS-35-60	CSSW	60	5000
CS-35-90	CSSW	90	5000
CS-36-30	CSSW	30	6000
CS-36-45	CSSW	45	6000
CS-36-60	CSSW	60	6000
CS-36-90	CSSW	90	6000

4. COMPARISON OF CS AND SS SPECIMEN

Due to high in-plane stiffness and strength of steel plate, attention should be paid to ensure that the steel plate yield prior to the yield of boundary beams or columns. The seismic input energy is mainly dissipated through the inelastic deformation of the steel plate. The boundary columns and boundary beams are designed to keep elastically as long as possible. By this arrangement, the system is able to maintain stability even after the failure of the shear panel.

Fig.6 indicates the energy absorption of specimens. Result shows that the fiber polymer is increased the energy absorption ability of the steel shear wall.

In practice, when lateral loads are applied to the structure, the structure undergoes an additional moment. The additional displacement imposes a greater internal moment to neutralize the moment created by vertical loads. If the structure is flexible and gravitational loads are high enough, in the critical condition, the additional loads generated by the $P-\Delta$ effect may increase the stress above the allowable limit in some components and by making instability, could to lead the structure failure. Thus, the use of load resisting systems which have more stiffness and less lateral displacement under lateral load is efficient. The capacity, elastic stiffness and over strength value of specimens have been listed in table 4. Values of this table are shown that the fiber polymer is increased the capacity and the elastic stiffness and over strength factor. Therefore the CFRP is effective to improve the steel shear wall behavior against seismic loads.

Also Results of test showed, the existence of the CFRP composite does not get involve in energy transfer of the frame, however it contributes positively in stress distribution over the steel plate. This involvement and distribution will have an increasing effect as the steel plate deformation progresses.

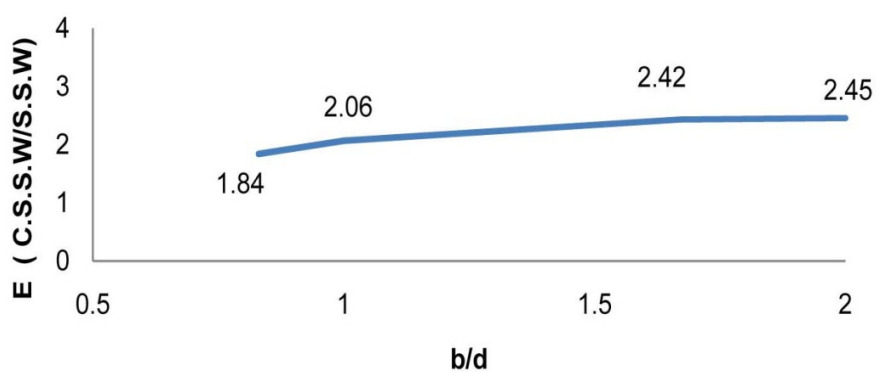


Fig. 6 Energy absorption ratio diagram

Table 4 capacity, stiffness value

Specimen	S-33	S-35	S-36	CS-33	CS-35	CS-36
Capacity (KN)	5669.5	7356.2	8260.14	18437.4	16583	25600
$K_{elastic}$ (KN/mm)	637.02	835.93	917.79	1084.55	1005.03	1422.22
Ω	2.36	2.41	2.57	4.61	2.83	3.59

5. ANALYSIS OF CFRP-COMPOSITE SHEAR WALL

5.1. Basic Assumptions

A typical story of a multistory structure with composite steel shear wall can be represented as an isolated panel for which the following assumptions can be made:

- The columns are rigid enough to neglect their deformation when calculating the shear deflection of the steel plate.

- The difference in tension-field intensity in adjacent stories is small and therefore bending of the floor beams due to the action of the tension field is neglected (Sabouri-Ghomi 2005).
- The steel plate can be considered as simply supported along its boundaries.
- The effect of stress due to flexural behavior (global bending stresses) on shear buckling stress of the steel plate is neglected.
- The principle of superposition applies.
- In CFRP-Composite steel shear wall, a layer of CFRP is increased the number of diagonal tension fields lines.

5.2. Load-Displacement calculation

The following, procedure describes the proposed method to analysis and design a CFRP-composite steel shear wall. Equations used in the proposed method are listed Eq (7) to Eq (17) and are explained in detailed in Fig 7, 8, 9.

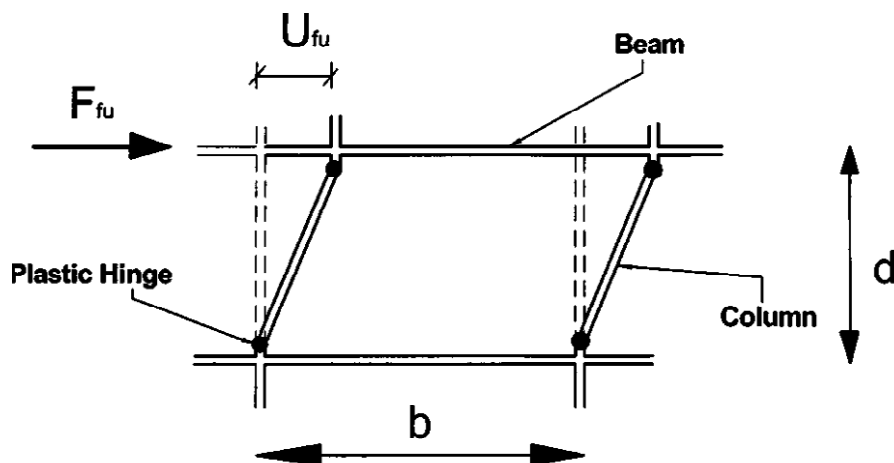


Fig. 7 Frame idealization (Sabouri-Ghomi 2005)

It is assumed that the beam–column connections are fixed and the beams behave as rigid elements. Point A is defined in Fig. 9 by obtaining F_{fu} and U_{fe} from Eq (7) and Eq(8). The slope of line OA in Fig. 9 is the stiffness of the frame. Then the load–displacement diagram of the frame will be defined. The shear strength and shear displacement and shear stiffness of the frame are (Sabouri-Ghomi 2005):

$$F_{fu} = \frac{4.M_{pf}}{d} \quad (7)$$

$$U_{fe} = \frac{M_{pf}.d^2}{6EI_f} \quad (8)$$

$$K_f = \frac{24EI_f}{d^3} \quad (9)$$

Point B is calculated using the Eq. (10) to Eq. (14). Shear displacement (in-plane displacement) of steel plate and CFRP sheet is equal. It is idealized from parallel springs principle. It is used from this principle to calculate of shear strength and displacement of steel sheet that have been covered by CFRP. Therefore Eq. (10) until Eq. (14) proposed by blend of PFI method (Sabouri-Ghomi 1992), parallel springs principle, numerical results, classic equations of shell and plate, investigation of sandwich panel behavior, several factors experiments. Experimental and numerical study showed that the layers of CFRP is increased the number of diagonal tension fields lines and elastic buckling of steel plate. Therefore its influence on shear buckling and shear strength of system, have been used.

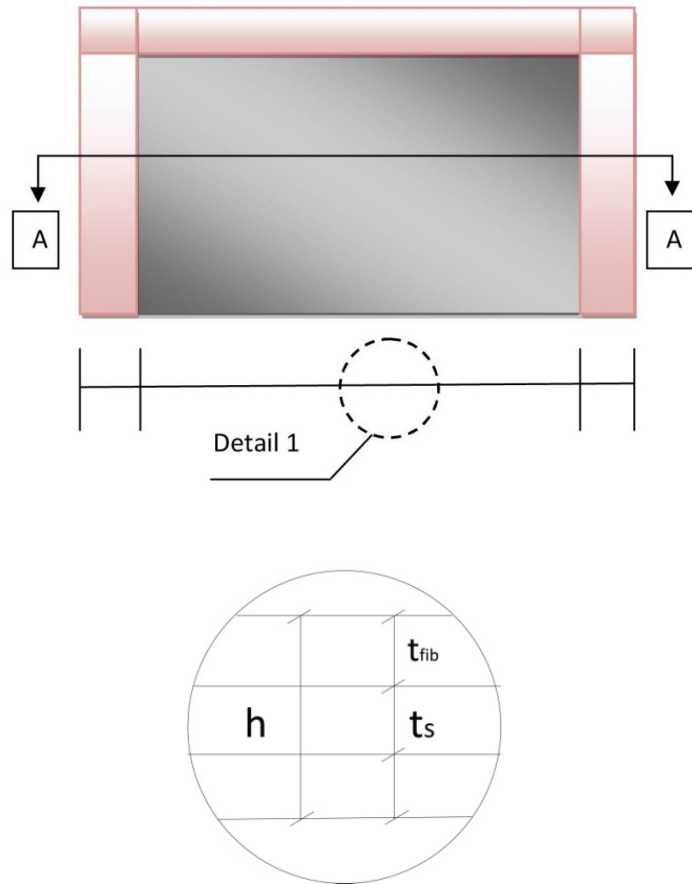


Fig. 8 CFRP-Composite steel shear wall

$$\tau_{cr} = \frac{K \cdot \pi^2}{b^2 \cdot t} \cdot D \quad (10)$$

$$D = \frac{E_s \cdot t_s^3}{12(1-\theta^2)} + 1.5(t_{Fib} \cdot h) \cdot (2E_1 + \frac{G_{12}}{2}) \quad (11)$$

$$F_{tw} = \tau_{cr} \left(1 + \sqrt{6.75 + \frac{F_{ys}}{\tau_{cr}}} \right) \quad (12)$$

$$U_w = \left(\frac{\tau_{cr}}{G_s} + \frac{2F_{tw}}{E_s} \right) \cdot d \quad (13)$$

$$F_w = (\tau_{cr} + 0.5F_{tw})b \cdot t \quad (14)$$

The shear load–displacement diagrams for the plate and the surrounding frame can be obtained separately. Then, by superimposing the two shear load–displacement diagrams that of the panel can be obtained. By using Von Misses yield criterion, this stress distribution provides a lower bound for the strength of the web plate, provided that the surrounding frame members are strong enough to sustain the normal boundary forces associated with the tension field. Point C and D calculate by using the Eq. (15), to Eq. (17).

$$F_p = K_f \cdot U_w + F_{wu} \quad (15)$$

$$K = F_p / U_w \quad (16)$$

$$F_C = F_{fu} + F_{wu} \quad (17)$$

Diagram in Fig. 9 is proposed to calculate other load-displacement points. With refer to Fig. 9, Point E and F also obtain. In this diagram the load-displacement slop (stiffness) change in $\Delta=0.005d$ and $\Delta=0.015d$.

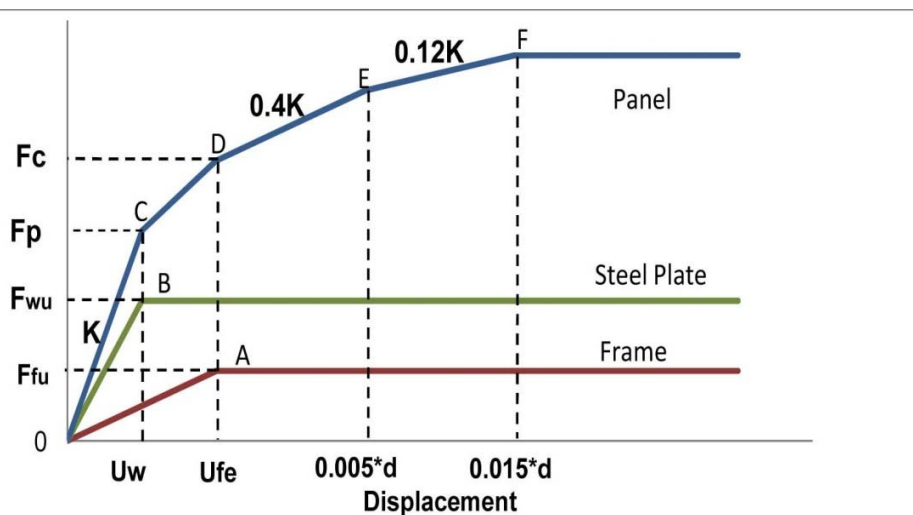
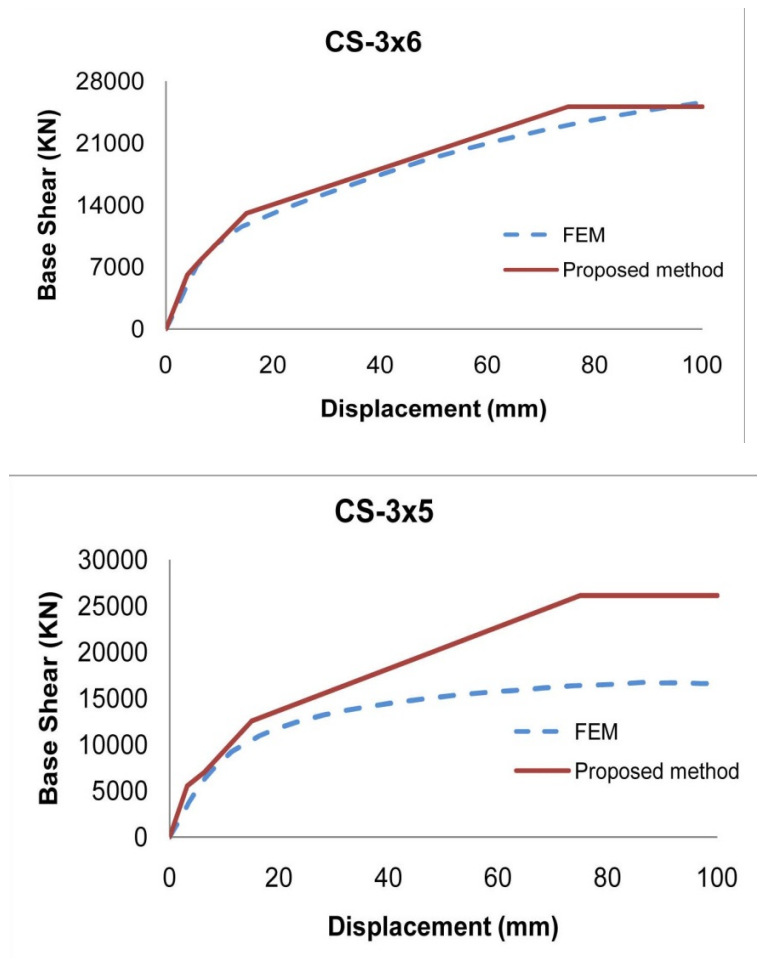


Fig. 9 Load-displacement diagram

In the Fig. 10, results of proposed method with FEM modeling have been compared. The results show convergence between of them. Proposed method estimate the CFRP-composite steel shear walls in elastic and inelastic zone. This comparison exhibit a good convergence between the proposed method with FEM results.



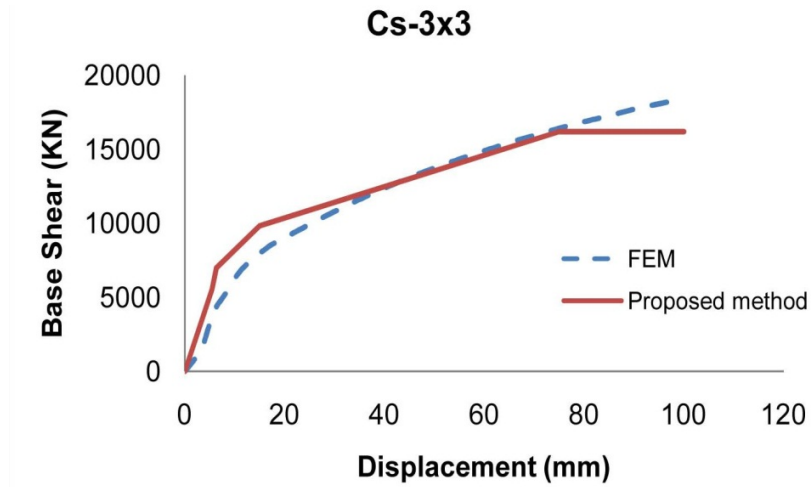


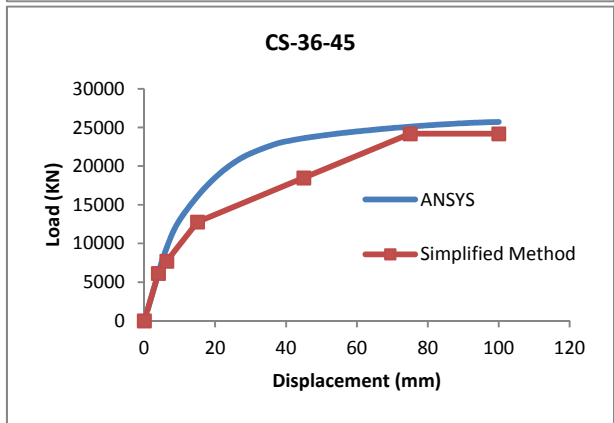
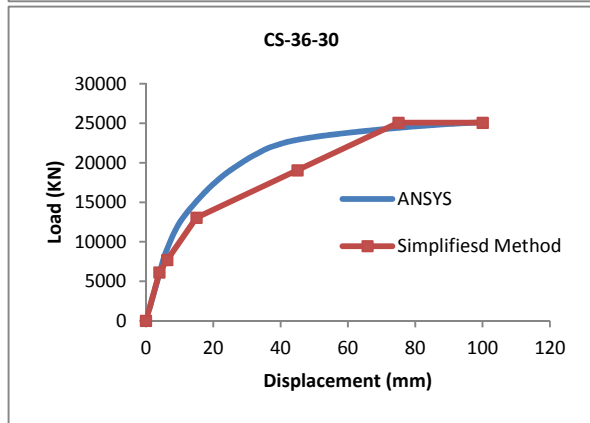
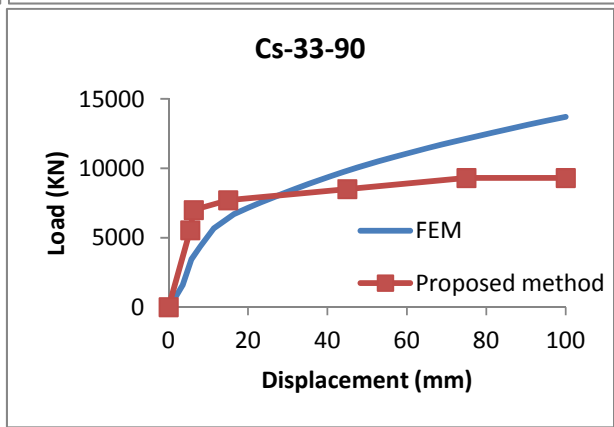
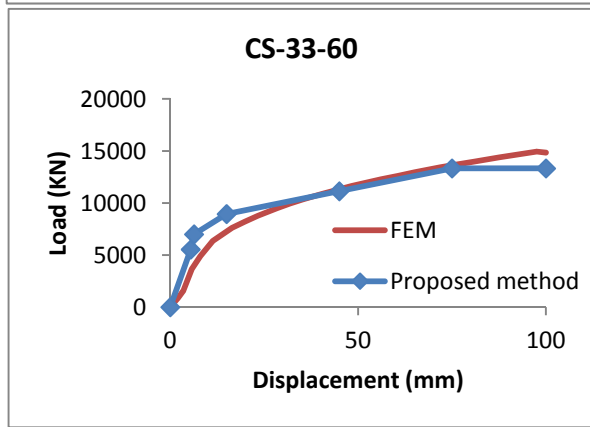
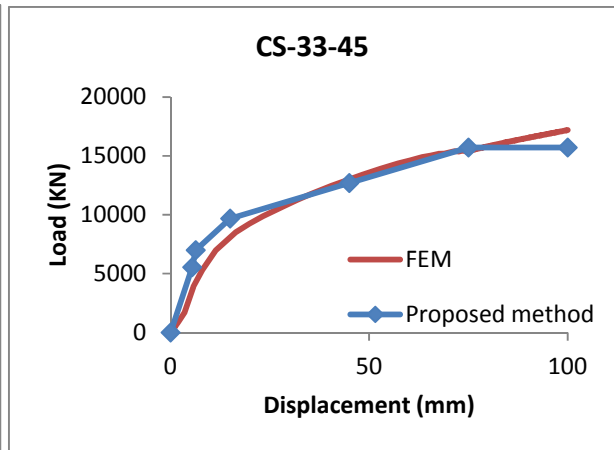
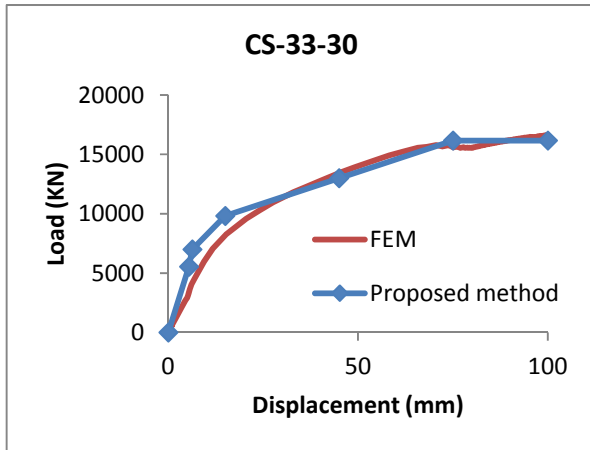
Fig. 10 Results comparison of proposed method & FEM

5.3. Influence Of Fiber Angle

For draw the load-Displacement curve with different angles of CFRP, only K is modified. The K modified is proposed as the following:

$$K\theta = \left(\frac{\theta \exp^4}{10000000} - \frac{\theta \exp^3}{200000} + 0.001\theta \exp^2 - 0.0148\theta + 1 \right) K \quad (18)$$

Eq. (18) obtained from fitness of specimens results. In the Fig. 11, results of FEM (ANSYS program) & proposed Method (Simplified) have been compared.



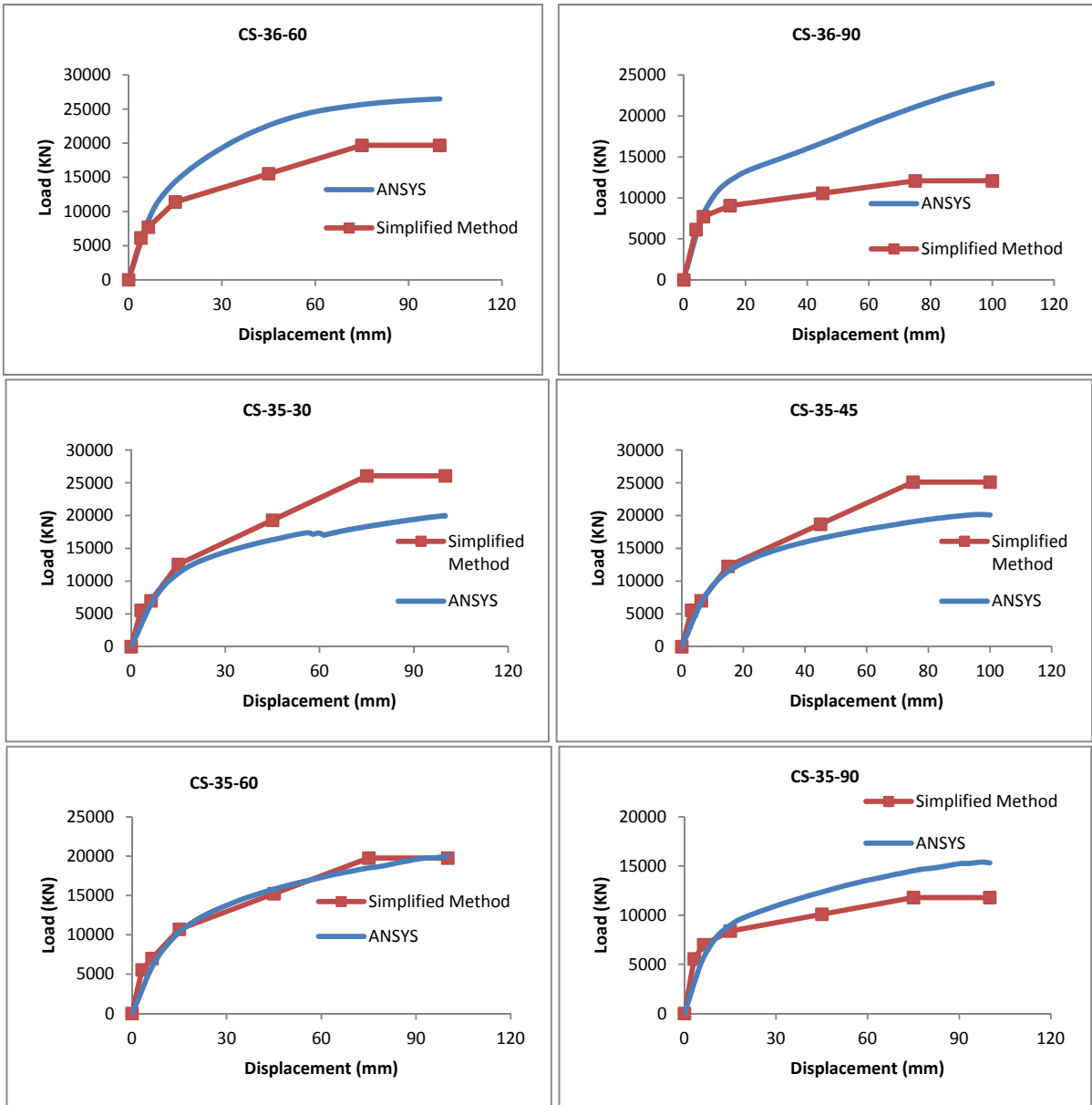


Fig. 11 Results comparison proposed method & FEM

6. CONCLUSION

The conclusions drawn from the experimental and numerical investigations on the effect of CFRP on the SSW may be summarized as follows;

1. The CFRP enhances the structural parameters such as; elastic stiffness, the shear capacity and the over strength values. It is concluded that the CSSW is an effective system against lateral loads.
2. The stiffness values to decrease more in the SSWs compared to the CSSWs and improves behavior of the SSW stiffness in the inelastic zone.
3. An analytical model has been proposed to predict the CSSW with variant polymer angle.
4. For draw the load-Displacement curve with different angles of CFRP, only the stiffness is needed to modify.
5. Finally, some equations have been suggested to calculate the nonlinear behavior of the CSSW system using the elastic analysis.

References

Bryan. GH, (1891),” On the stability of a plane plate under thrusts in its own plane with applications on the buckling of the sides of a ship”, Proceedings of London Mathematical Society.

Timoshenko. SP, Gere. JM, (1947),” Theory of elastic stability”, 2nd ed. NY: McGraw-Hill; 1961. Stein MN. NACA tech. note no 1222.

Bruhn. EF,(1973),” Analysis and design of flight vehicle structures”, 1st ed, Tri-State Offset Company.

Allen. H, Bulson. P, (1980),” Background to buckling, McGraw Hill.

Maquoi R, Skaloud M,” Stability of plates and plated structures, general report”, Journal of Constructional Steel Research 2000;55:45–68.

Lee SC, Davidson JS, Yoo CH,” Shear buckling coefficients of plate girder web panels”, Computers and Structures 1996;59(5):789–95.

Lee SC, Yoo CH, Yoon DY, "Behaviour of intermediate transverse stiffeners attached on web panels", Journal of Structural Engineering ASCE 2002;128(3):337–45.

Bradford MA, "Improved shear strength of webs designed in accordance with the LRFD specifications", Engineering Journal 1996;33(3):95–100.

Paik JK, Thayamballi AK, "Buckling strength of steel plating with elastically restrained edges", Thin-Walled Structures 2000;37:27–55.

Lubell AS, Prion GL, Ventura CE, Rezai. M, "Unstiffened steel plate shear wall performance under cyclic loading", Journal of Structural Engineering ASCE 2000;126(4):453–60.

S. Sabouri-Ghomi, C.E. Ventura, M.H. K. Kharrazi, "Shear Analysis and Design of Ductile Steel Plate Walls", JOURNAL OF STRUCTURAL ENGINEERING , 2005, pp. 879, 889

Mangonon, P.L. (1999), "The Principles of Materials Selection for Engineering Design", Prentice Hall.

ISIS Canada, (2001), "Reinforcing Concrete Structures with Fiber Reinforced Polymers", Manual, ISIS Canada Corporation, Winnipeg, Canada.

Wyckoff, R. (1964), "Crystal Structures", New York 1964, Vol. 1